Arm-Length Dependence of Stress Relaxation in Star Polymer Melts

S. T. Milner*

Exxon Research & Engineering, Route 22 East, Annandale New Jersey 08801

T. C. B. McLeish

Department of Physics and Astronomy, University of Leeds, Leeds LS29JT, England

Received January 20, 1998

ABSTRACT: We apply our recent microscopic theory of stress relaxation in star polymer melts to dynamic rheology data of Fetters et al. on melts of monodisperse four-arm polyisoprene stars, with arm molecular weights in the range 17 000 to 105 000 (M/M_e from 3.4 to 21.0, with $M_e = 5000$). The agreement between theory and experiment is excellent for all frequencies and arm lengths, with physically reasonable values of plateau modulus and friction factor and no other adjustable parameters. These data obey time−temperature superposition, with no evidence for anomalous arm-length dependence of activation energies as seen in polyethylene-branched polymers.

Recently, we have presented a microscopic theory of stress relaxation in monodispserse star polymer melts,[1] based on concepts of arm retraction[2,3] and "dynamic dilution",[4] which gave excellent agreement without free parameters to dynamic rheology data on star melts. As a further and more stringent test of this theory, here we make comparisons between our theory and dynamic rheology of a set of seven polyisoprene (PI) four-arm star melts synthesized and studied by Fetters et al.,[5] in which the arm molecular weights M_a vary from 17 000 to 105 000.

This extensive data set serves as a stronger test of the theory than was performed in ref 1 because the terminal times of these melts vary over 5 orders of magnitude as M_a increases. A correct theory should reproduce this variation, and indeed the systematic variation of the shapes of $G'(\omega)$ and $G''(\omega)$ as M_a increases, without recourse to artificial fitting parameters.

The chemical system of polyisoprene is particularly well suited for such a study, because of (1) the availability of anionically synthesized star polymers, (2) the available variation of rheological time scales over a wide, convenient temperature range; and perhaps most importantly (3) the experimental validity of time−temperature superposition in polyisoprene, even for stars and other branched polymers. Polybutadiene is likewise a convenient choice for similar reasons.

In contrast, some polymer systems, most notably polyethylene (PE), have been shown to have "activation energies" E_a (operationally defined as the slope d log τ/d(1/T) in some temperature range) that for star polymers vary linearly with M_a. Graessley and Raju[6] observed a variation of $E_a(M_a) = 7.2 + 0.28M_a/M_c$ kcal/mol, the "crossover" molecular weight M_c for polyethylene is about 3800; note that the short-arm limit of $E_a(M_a)$ is $E_a^{linear} = 7.2$ kcal/mol, which is the observed value for linear chains.

More precisely, time−temperature superposition fails for these systems; the behavior may be described by a frequency-dependent $E_a(\omega)$, equal to E_a^{linear} at high frequencies and smoothly increasing to a greater value $E_a(M_a)$ at lower frequencies of order the inverse of the terminal time. This behavior in PE and other such systems is not completely understood, but for present purposes it suffices to remark that PI does not show this behavior (as we will explicitly demonstrate below).

The experimental system of ref 5 presents another advantage for testing the theory, namely that aliquots of the anionically synthesized star arms were extensively characterized prior to being linked together to form a star, in addition to characterization of the completed star. Thus the molecular weights of the star arms are well-known experimentally. Because the stress relaxation in star melts is a strong, exponential function of the arm molecular weight, modest errors in determining M_a can lead to large discrepancies in the theoretically predicted and experimentally measured rheology.

We now present a summary of the stress relaxation theory for star melts; for details see ref 1.

As for any entangled polymer melt, stress in a star polymer melt is stored in anisotropic chain conformations. Stress after a step strain persists until chains are able to explore new conformations; the decay of stress after a step strain $\sigma(t) = G(t)\epsilon$ is equivalent to the dynamic modulus $G(\omega)$ by Fourier transform.

As in linear melts, we represent the entangling effect of other chain segments on a given star arm in terms of a confining "tube". The tube diameter a is a phenomenological material parameter; a chain segment of the entanglement molecular weight M_e has a radius of gyration of order a.

Because the arms of a star are joined at a common point, they cannot reptate as linear chains do to explore new conformations. Instead, as pointed out by Helfand and Pearson,[3] they must retract within their tubes and poke out along a new direction. A star arm may retract its free end partway toward the junction point and thus renew only part of the arm conformation near the free end when the arm pokes out again. Retraction occurs in each arm independently, with the striking consequence that the entire dynamic rheology of multiarm stars for number of arms $f > 4$ is observed to be the same, independent of f (and with only 30% variations for $f = 3$).[3]

The process of arm retraction is entropically unfavorable, because the retracted conformations have many

10.1021/ma980060d CCC: $15.00
Published on Web 10/02/1998

loops along which the arm is obliged to double back on its own path. Thus there is a free energy barrier to retraction, which is increasingly large for deeper retractions. Reference 3 computed the corresponding barrier potential $U(s)$ for retraction a fractional distance s ($0 < s < 1$, with $s = 0$ at the free end) down the tube for a star arm in a fixed network of entanglements, which turns out to be

$$U(s) = (15/8)(M_a/M_e)s^2 \qquad (1)$$

where M_a is the arm molecular weight.

The barrier to full retraction (free end retracts to the junction point, and the entire arm conformation is renewed) $U(1)$ is then exponential in the length of the arm, which leads to very long terminal times for star melts with modest arm lengths, as well as a very broad spectrum of relaxation times corresponding to partial arm retraction.

Because the spectrum of relaxation times is so broad, on the time scale for retraction $\tau(s)$ to a fractional distance s down the tube, chain segments with $s' < s$ have relaxed many times over. Thus only those chain segments with $s' > s$, with volume fraction $\phi = 1 - s$, are effective at topologically confining segments at s; the rest should be regarded as absent from the entangling network on the time scale $\tau(s)$. This "dynamic dilution"[4] dramatically speeds up arm retraction in a star melt as compared to a star arm in a fixed network. Dynamic dilution implies a dilated tube diameter and a larger effective value of M_e on the time scale $\tau(s)$. Naively, we might expect M_e to be replaced by $M_e(\phi) = M_e(1)/\phi$, if we think of entanglements as binary events and count the arc length along a given strand between successive effective entanglements as M_e. Because the plateau modulus G_0 of an entangled melt is roughly k_BT per entanglement volume, this would imply a plateau modulus for a diluted network with volume fraction ϕ scaling as f^2. In fact, careful experiments on plateau moduli in Θ solutions[7] as well as a more sophisticated scaling argument[8] imply that the diluted modulus scales as $\phi^{7/3}$, corresponding to

$$G(\phi) = G_0\phi^{1+\alpha} \qquad M_e(\phi) = M_e(1)/\phi^{\alpha} \qquad (2)$$

with $\alpha = 4/3$.

Arm retraction may be regarded as a hierarchical process, in that the time scale $\tau(s)$ for retraction a fractional distance s ($0 < s < 1$) down the tube sets the attempt frequency for retraction to $s + \Delta s$, while the potential difference $U(s + \Delta s) - U(s)$ sets the barrier for it. In the differential limit this becomes[4]

$$\frac{\mathrm{d}}{\mathrm{d}s} \ln \tau(s) = \frac{\partial U}{\partial s}(s;\, N_e(s)) = \frac{\mathrm{d}U_{\mathrm{eff}}}{\mathrm{d}s}(s) \qquad (3)$$

Here we have defined a new potential $U_{\mathrm{eff}}(s;\alpha)$ by

$$U_{\mathrm{eff}}(s;\alpha) = (15/4)(M_a/M_e)\,\frac{1 - (1-s)^{1+\alpha}[1 + (1+\alpha)s]}{(1+\alpha)(2+\alpha)} \qquad (4)$$

which for $\alpha = 1$ reduces to the expression in ref 4, namely $U_{\mathrm{eff}}(s) = (15/8)(M_a/M_e)(s^2 - 2s^3/3)$. Evidently, $\tau(s) \sim \tau_0 \exp(U_{\mathrm{eff}}(s))$, where τ_0 is some "microscopic" attempt frequency.

In addition to computing the "barrier" contribution to $\tau(s)$ for arm retraction, taking account of dynamic dilution with the Colby–Rubinstein scaling for $M_e(\phi)$, the theory of ref 1 includes two other ingredients, which we summarize here.

First, for sufficiently small values of s, arm retraction faces a barrier of less than k_BT, for which the estimate of $\ln \tau(s)$ from eq 3 is not accurate. Such small retractions occur at early times after an applied step strain and hence affect high-frequency dynamic response. The corresponding chain motions depend not only on the lowest collective retraction mode, but higher internal modes as well. We estimate the relaxation rate from these small retractions by studying the motion of the end of a semi-infinite Rouse chain in a tube. These relaxation processes cross over to the "activated" retraction at a time of order the Rouse time of the arm.

Second, in addition to computing the barrier for arm retraction, Ref 1 computes the attempt frequency [the prefactor to $\exp(U_{\mathrm{eff}}(s))$] by defining a first-passage time problem, for the free end of a star arm diffusing "uphill" in the potential $U_{\mathrm{eff}}(s)$ to reach a given value $s = s_f$ starting at $s = 0$. This one-dimensional steady-state diffusion problem can be solved exactly in terms of integrals over U_{eff}; the resulting mean first-passage time is the product of a factor $\exp(U_{\mathrm{eff}}(s_0))$ and another factor that can be interpreted as the inverse of the attempt frequency. A similar procedure is outlined in ref 9.

The time-dependent modulus is calculated for the melt of stars as a sum of contributions from each segment along the arms. The segment at s is taken to relax with a characteristic time $\tau(s)$.

The amount by which the modulus decreases on a time scale $\tau(s)$ is simply the increment $\partial G(\phi(s))/\partial s\ \mathrm{d}s$, with the entangled volume fraction given by $\phi(s) = 1 - s$; using eq 2, this results in

$$G(t) = G_0(1+\alpha)\int_0^1 \mathrm{d}s\,(1-s)^{\alpha}\exp[-t/\tau(s)] \qquad (5)$$

(For the full expressions for $\tau(s)$, see the Appendix.) The dynamic modulus $G(\omega)$ is related as usual by Fourier transform to the time-dependent modulus as $G(\omega) = i\omega F[G(t)](\omega)$, so that

$$G(w) = G_0(1+\alpha)\int_0^1 \mathrm{d}s\,(1-s)^{\alpha}(-i\omega\tau(s))/(1 - i\omega\tau(s)) \qquad (6)$$

Because small variations in the value of M_a lead to large variations in the predicted rheology, we have taken the following approach in comparing the star theory to the PI data. For each of the seven data sets, we have chosen by hand a value of M_a/M_e that best fits the $G''(\omega)$ data. We shall examine below how these fitted values of M_a/M_e compare to the experimental values.

The shape of G'', with its broad range of relaxation process from the terminal time up to a peak, rather tightly restricts the best-fit value of M/M_e for each data set. Note that we have chosen values for τ_e and G_0 that are consistent with experimental values published elsewhere (the highest-M_a set of the present work is the same as the set of PI data in ref 1, where consistency of our values for τ_e and G_0 with literature values is shown). The results of this fitting are shown in Figure 1, where it is evident that the shapes of the spectra are well reproduced by the theory. The corresponding curves for

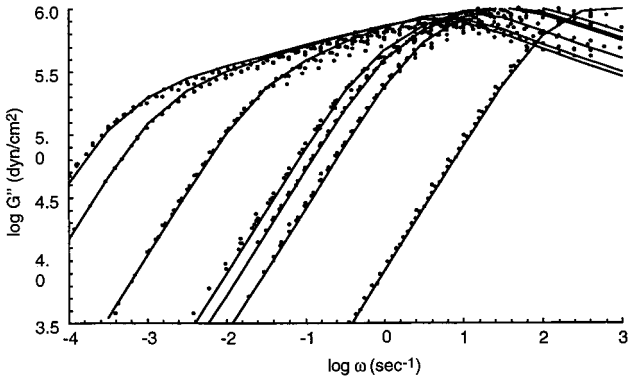

Figure 1. Time−temperature superposed data and theoretical predictions for $G''(\omega)$, for monodisperse polyisoprene four-arm stars with $10^{-3}M_a = 11.4$, 17, 36.7, 44, 47.5, 95, and 105 (which appear in the plot in order of increasing terminal time). The values of M_a/M_e for each sample have been adjusted to give the best fit to the data.

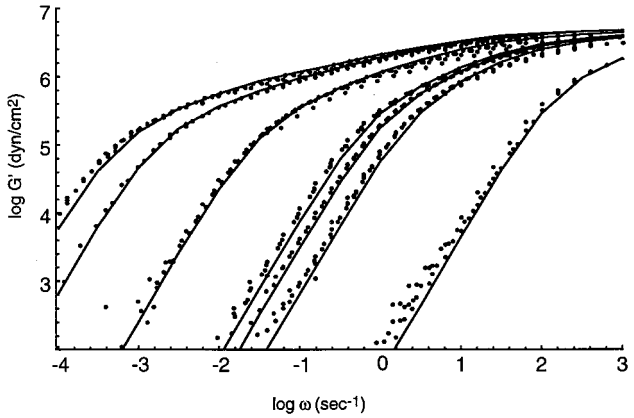

Figure 2. Time−temperature superposed data and theoretical predictions for $G'(\omega)$, for the samples and parameter values of Figure 1.

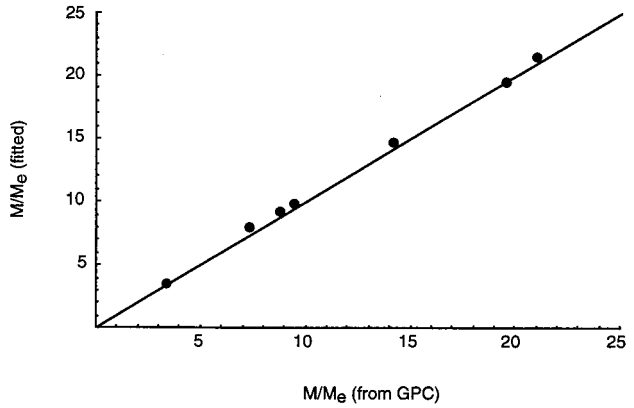

Figure 3. Fitted values of M_a/M_e from Figure 1 plotted versus the experimental values (from GPC of the arm precursor, with $M_e = 5000$), giving a straight-line fit with slope 1.0 through the origin.

$G'(\omega)$ are shown in Figure 2, which are also in good agreement with the data.

Now we compare in Figure 3 the fitted values of M_a/M_e to the experimentally measured values, from gel permeation chromatography performed on the star arms before joining them into a star.[5] (Reference 5 takes $M_e = 5000$ g/mol for PI.) We find the hoped-for result; namely, the fitted and measured values are the same to within the scatter in the measured values. The least-squares line through the data has slope 1.0 and passes

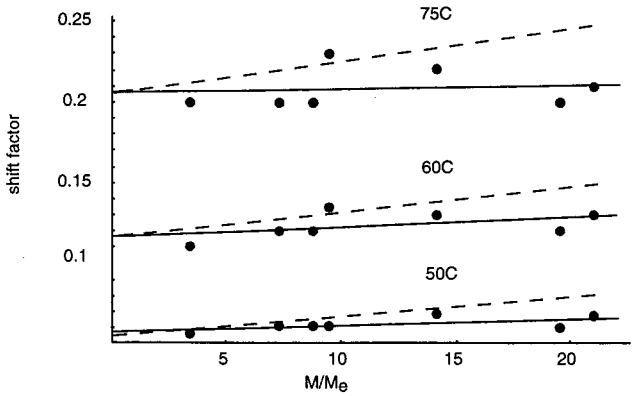

Figure 4. Time−temperature frequency shift factor values plotted versus M_a/M_e for temperatures 50, 60, and 75 °C, showing no linear increase with M_a/M_e. The dashed lines are the predicted variation of shift factors based on the claimed results of ref 10; the solid lines are least-squares fits to the data.

essentially through the origin. This demonstrates strong agreement between the data and the theory, over a wide range of frequency and now M_a/M_e in a single system.

We have also repeated this entire exercise with the theory modified to give the naive "dilution exponent" of $G(\phi) = G_0\phi^\alpha$ with $\alpha = 2$ rather than the Colby−Rubinstein result[8] of $\alpha = 7/3$. With that assumption, we are able to obtain fits to G'' and G' of comparable quality to those in Figures 1 and 2, with different fitted values of M_a/M_e. The comparison of the corresponding fitted and experimental values of M_a/M_e then reveals once again a straight line through the origin, but this time with a slope of about 0.7. Simply put, the value of M_e would have to be increased by about 30% (i.e., 5000 replaced by 6500) for the theory with dilution according to $G(\phi) = G_0 f^2$ to agree with the data. Such a large increase in M_e would be inconsistent with the values extracted from measurements of the plateau modulus in high molecular weight monodisperse linear PI melts.[10]

Finally, we return to our assertion above that the PI star data obey time−temperature superposition, unlike some systems such as PE,[6] and in contradiction to some published reports.[11] In ref 11, three different three-arm PI stars were studied, with total molecular weights of 284 000, 342 000, and 854 000; excess activation energies $\Delta E_a \equiv E_a - E_a^{\text{linear}}$ of 1.3, 2.3, and 3.2 kcal/mol were reported. Anticipating a linear variation of $E_a(M_a)$ as in ref 6, we fit these three points to a straight line through the origin to obtain $\Delta E_a = 0.063M_a/M_e$ (the three points are somewhat scattered about this line, but this captures the magnitude of the claimed effect).

Using the unshifted raw data (taken at temperatures 25, 50, 60, and 75 °C) from ref 5, we performed time−temperature shifts of the higher-temperature data back to 25 °C by hand to obtain the master curves shown in Figures 1 and 2. The corresponding shift factors as a function of M_a/M_e are shown in Figure 4; the straight lines are least-squares fits to these data sets, and the dashed lines show the M_a/M_e dependence predicted by our analysis above of the ref 11 results. The shift factor values scatter about essentially horizontal lines and appear to be inconsistent with the magnitudes of ΔE_a reported in ref 11.

In conclusion, the present comparison of our microscopic theory for stress relaxation in star polymer melts to the extensive polyisoprene data set from the work of

Fetters et al.[5] shows that the theory is in quantitative agreement with experiment, with a reasonable value for the entanglement molecular weight M_e of about 5000 (and reasonable values for the friction factor and plateau modulus as well[1]), and no adjustable parameters. The theory, reported in detail in ref 1, depends crucially on concepts of arm retraction within a "tube" representing the entanglements with other chains, and the "dynamic dilution" effect of faster-relaxing chain segments being progressively removed from the entangling matrix on slower time scales. As such, the quantitative success of this theory in explaining stress relaxation in star polymer melts, for which there are at present no competing theories, represents in some sense a stronger verification of the tube concept even than experiments on reptation in linear polymers.

Acknowledgment. We thank Lew Fetters for making available the original data sets from ref 5 and Bill Graessley and Michael Rubinstein for many stimulating and enjoyable discussions.

Appendix

Here we summarize the detailed results of ref 1 for the relaxation time $\tau(s)$.

In the early-time or high-frequency "Rouse retraction" regime, the motion of the arm free end down the tube is governed by the longitudinal (along the tube) Rouse modes of a semi-infinite chain. The free end does not yet feel the effect of the branch point, and so the mean-square displacement of the end along the tube $z^2(t)$ in this regime is independent of arm length. The mean-square fluctuations of the end location grow with time, as lower Rouse modes with longer relaxation times contribute. At the Rouse time $\tau_R = \tau_e(N/N_e)^2$, $z^2(t)$ is of order the arm end-to-end radius $R^2 = Nb^2$, and the chain free end "discovers" that it is not infinite.

This leads to a scaling result $z^2(t) = R^2(t/\tau_R)^{1/2}$: a simple calculation using the Rouse model fixes the coefficient. Relating distance down the tube z to fractional distance s by $z/L = s$ in terms of the tube length L (which satisfies $La = R^2$) and inverting the scaling relation above, we find

$$\tau_{early}(s) = 225\pi^3/256\tau_e(N/N_e)^4 s^4 \tag{7}$$

with τ_e the Rouse time of an entanglement segment, $\tau_R = \zeta N^2 b^2/(3\pi^2 k_B T) = \tau_e(N/N_e)^2$.

Note that we have computed the relaxation time $\tau_{early}(s)$ using the mean-squared displacement of the free end, rather than defining a mean first-passage time as we do for deeper retractions. One reason for this is that the distribution of first-passage times of a random walker to an absorbing barrier does not have a finite first moment $\langle t \rangle$ (lower moments such as $\langle 1/t \rangle$ do exist). Depending on the precise definition of $\tau_{early}(s)$ we make, the prefactor in eq 7 would presumably change, which would lead to small changes in the shape of the dynamic spectra at high frequencies.

At later times or lower frequencies, in addition to computing the barrier for arm retraction, ref 1 computes the attempt frequency [the prefactor to $\exp(U_{eff}(s))$] by defining a first-passage time problem, for the free end of a star arm diffusing "uphill" in the potential $U_{eff}(s)$ to reach a given value $s = s_f$ starting at $s = 0$.

The steady-state probability distribution $P(z)$ for the free-end position for $z < 0$ (i.e., from the equilibrium free-end position $z = 0$ to some $z = z_f < 0$ in the direction of the branch point) satisfies a Fokker−Planck equation with a steady current J_{in} injected at $z = 0$,

$$-J_{in} = D_{eff}\frac{\partial}{\partial z}\left(\frac{\partial P}{\partial z} + P\frac{\partial U}{\partial z}\right) \tag{8}$$

(For $z > 0$, $P(z)$ is simply the equilibrium distribution, since no current flows in that direction.)

In terms of $P(z)$ and J_{in}, the mean first-passage time from $z = 0$ to $z = z_f$ can be written as the mean number of "walkers" (injected ends) present in steady state, divided by the number per unit time injected:

$$\bar{\tau}(z_f) = J_{in}^{-1}\int dz\, P(z) \tag{9}$$

Equation 8 can be solved exactly in terms of integrals over U_{eff}; using equation 9, the resulting mean first-passage time is the product of $\exp(U_{eff}(s_0))$ and a second factor that can be interpreted as the inverse of the attempt frequency.

After some algebra and approximations we find[1]

$$\tau_{late}(s) \approx \tau_e\left(\frac{N}{N_e}\right)^{3/2}\left(\frac{\pi^5}{30}\right)^{1/2} \frac{\exp[U_{eff}(s)]}{s\left[(1-s)^{2\alpha} + \left(\left(\frac{4N_e}{15N}\right)(1+\alpha)\right)^{2\alpha/\alpha+1}\Gamma\left(\frac{1}{\alpha+1}\right)^{-2}\right]^{1/2}} \tag{10}$$

(This is eq 29 of ref 1 with an additional factor of 1/2, which was mistakenly omitted in the earlier paper.)

The early-time and late-time results equations 7 and 10 are joined together for our calculations in a simple crossover formula,

$$\tau(s) \approx \frac{\tau_{early}(s)\exp[U_{eff}(s)]}{1 + \exp[U_{eff}(s)]\tau_{early}(s)/\tau_{late}(s)} \tag{11}$$

(which was incorrectly rendered in eq 22 of ref 1).

This crude crossover form works because $\tau_{early}(s)$ goes as $\tau_e s^4(N/N_e)^4$ and $\tau_{late}(s)\exp[-U_{eff}(s)]$ goes as $\tau_e(N/N_e)^{3/2}/s$ for small s. We want to cross between $\tau_{early}(s)$ and $\tau_{late}(s)$ at $s \sim (N_e/N)^{1/2}$. Note that for $s \ll (N_e/N)^{1/2}$, we have $\tau_{late}\exp[-U_{eff}] \gg \tau_{early}$, and eq 11 reduces to $\tau_{early}(s)\exp[U_{eff}]$; but for such small s the factor $\exp[U_{eff}] \approx 1$. On the other hand, for $s \gg (N_e/N)^{1/2}$ we have $\tau_{late}\exp[-U_{eff}] \ll \tau_{early}$, and eq 11 reduces to $\tau_{late}(s)$.

References and Notes

(1) Milner, S. T.; McLeish, T. C. B. *Macromolecules* **1997**, *30*, 2159.
(2) de Gennes, P. G. *J. Phys. Fr.* **1975**, *36*, 1199.
(3) Pearson, D. S.; Helfand, E. *Macromolecules* **1984**, *17*, 888.
(4) Ball, R. C.; McLeish, T. C. B. *Macromolecules* **1989**, *22*, 1911.
(5) Fetters, L. J.; Kiss, A. D.; Pearson, D. S.; Quack, G. F.; Vitus, F. J. *Macromolecules* **1993**, *26*, 647.
(6) Graessley, W. W.; Raju, V. R. *J. Polym. Sci., Polym. Symp.* **1984**, *71*, 77.
(7) Adam, M.; Delsanti, M. *J. Phys. Fr.* **1984**, *45*, 1513.
(8) Colby, R. H.; Rubinstein, M. *Macromolecules* **1990**, *23*, 2753.
(9) Yurasova, T. A.; McLeish, T. C. B.; Semenov, A. N. *Macromolecules* **1994**, *27*, 7205.
(10) Fetters, L. J.; Lohse, D. J.; Richter, D.; Witten, T. A.; Zirkel, A. *Macromolecules* **1994**, *27*, 4639.
(11) Bero, C. A.; Roland, C. M. *Macromolecules* **1996**, *29*, 1562.

MA980060D